Protein Boson Peak Originated from Hydration-Related Multiple Minima Energy Landscape

ARTICLE *in* JOURNAL OF THE AMERICAN CHEMICAL SOCIETY · JULY 2005

Impact Factor: 12.11 · DOI: 10.1021/ja0425886 · Source: PubMed

3 AUTHORS, INCLUDING:

Akio Kitao
The University of Tokyo
95 PUBLICATIONS **2,527** CITATIONS
SEE PROFILE

Nobuhiro Go
Japan Atomic Energy Agency
238 PUBLICATIONS **9,848** CITATIONS
SEE PROFILE

J|A|C|S
ARTICLES
Published on Web 05/25/2005

Protein Boson Peak Originated from Hydration-Related Multiple Minima Energy Landscape

Yasumasa Joti,[†,‡] Akio Kitao,*[,§] and Nobuhiro Go[†,#]

Contribution from the Neutron Science Research Center, Japan Atomic Energy Research Institute, 8-1 Umemidai, Kizu-cho, Souraku-gun, Kyoto 619-0215, Japan, Institute of Molecular and Cellular Biosciences, The University of Tokyo, 1-1-1 Yayoi, Bunkyo-ku, Tokyo 113-0032, Japan, and Graduate School of Information Science, Nara Institute of Science and Technology, 8916-5 Takayama-cho, Ikoma, Nara 630-0101, Japan

Received December 9, 2004; E-mail: kitao@iam.u-tokyo.ac.jp

Abstract: The boson peak is a broad peak found in the low-frequency region of inelastic neutron and Raman scattering spectra in many glassy materials, including biopolymers below ~200 K. Here, we give a novel insight into the origins of the protein boson peak, which may also be valid for materials other than proteins. Molecular simulation reveals that the structured water molecules around a protein molecule increase the number of local minima in the protein energy landscape, which plays a key role in the origin of the boson peak. The peak appears when the protein dynamics are trapped within a local energy minimum at cryogenic temperatures. This trapping causes very low frequency collective motions to shift to higher frequencies. We demonstrate that the characteristic frequency of such systems shifts higher as the temperature decreases also in model one-dimensional energy surfaces with multiple minima.

Introduction

Neutron scattering spectra of systems that obey the Debye squared frequency law should be constant against frequency in the lowest frequency range. The boson peak is characterized by an excess spectral density of states as compared to the Debye frequency law. It is found in the low-frequency region (15−40 cm^{-1}) of inelastic neutron and Raman scattering spectra in many glassy materials, such as glass-forming liquids,[1] polymers,[2] and biological macromolecules,[3−8] at cryogenic temperatures below ~200 K. A peak corresponding to the boson peak has also been found in simulation studies of hydrated proteins.[9,10] As the temperature increases, the boson peak shifts to lower frequency and becomes buried in the quasi-elastic contributions. The boson peak is observed in such a wide range of glassy materials, including biopolymers, that attempts to clarify its origin have been pursued in fields ranging from physics to biology. The origin of the peak has been understood from a variety of viewpoints. For instance, it has been suggested for silica glasses that the peak is related to acoustic-like localized vibration[11] or to optic-like rotational motion.[12] In the case of fragile polymers, the vibration−relaxation crossover is proposed as the origin of the peak.[13] In simple liquids, the peak is explained by the mode-coupling theory.[14] The protein boson peak is claimed to be the result of accordion-like excitations of α-helices and β-sheets[15] or of similar localized motion in the molecule. In contrast, it is also suggested that the peak originates from protein motions extended over the entire protein molecule.[8] Despite both experimental[5,7,8] and theoretical[9,10] efforts, the origin of the protein boson peak has not yet been fully understood.

Another temperature-dependent phenomenon which has recently attracted much attention is a dynamical transition in proteins similar to the glass transition. This glasslike transition is observed as an abrupt increase in atomic fluctuations at a temperature above ~200 K and is accompanied by the disappearance of the boson peak.[4] The glasslike transition of proteins has been detected by a variety of experimental techniques, such as X-ray crystallography,[16] Mössbauer spectroscopy,[17] and incoherent neutron scattering.[4,18] It is suggested that below the transition temperature, a protein molecule is trapped in one of

[†] Neutron Science Research Center.
[‡] Current address: Institute of Molecular and Cellular Biosciences.
[§] Institute of Molecular and Cellular Biosciences.
[#] Graduate School of Information Science.

(1) Grigera, T. S.; Martin-Mayor, V.; Parisi, G.; Verrocchio, P. *Nature* **2003**, *422*, 289−292.
(2) Frick, B.; Richter, D. *Science* **1995**, *267*, 1939−1945.
(3) Cusack, S.; Doster, W. *Biophys. J.* **1990**, *58*, 243−251.
(4) Ferrand, M.; Dianoux, A. J.; Petry, W.; Zaccai, G. *Proc. Natl. Acad. Sci. U.S.A.* **1993**, *90*, 9668−9672.
(5) Diehl, M.; Doster, W.; Petry, W.; Schober, H. *Biophys. J.* **1997**, *73*, 2726−2732.
(6) Fitter, J. *Biophys. J.* **1999**, *76*, 1034−1042.
(7) Paciaroni, A.; Bizzarri, A. R.; Cannistraro, S. *Phys. Rev. E* **1999**, *60*, 2476−2479.
(8) Kataoka, M.; Kamikubo, H.; Yunoki, J.; Tokunaga, F.; Kanaya, T.; Izumi, Y.; Shibata, K. *J. Phys. Chem. Solids* **1999**, *60*, 1285−1289.
(9) Paciaroni, A.; Bizzarri, A. R.; Cannistraro, S. *Phys. Rev. E* **1998**, *57*, 6277−6780.
(10) Tarek, M.; Tobias, D. J. *J. Chem. Phys.* **2001**, *115*, 1607−1612.
(11) Foret, M.; Courtens, E.; Vacher, R.; Suck, J. B. *Phys. Rev. Lett.* **1996**, *77*, 3831−3834.
(12) Hehlen, B.; Courtens, E.; Vacher, R.; Yamanaka, A.; Kataoka, M.; Inoue, K. *Phys. Rev. Lett.* **2000**, *84*, 5355−5358.
(13) Buchenau, U.; Schonfeld, C.; Richter, D.; Kanaya, T.; Kaji, K.; Wehrmann, R. *Phys. Rev. Lett.* **1994**, *73*, 2344−2347.
(14) Götze, W.; Mayr, M. R. *Phys. Rev. E* **2000**, *61*, 587−606.
(15) Chou, K. C. *Biophys. Chem.* **1986**, *25*, 105−116.
(16) Rasmussen, B. F.; Stock, A. M.; Ringe, D.; Petsko, G. A. *Nature* **1992**, *357*, 423−424.
(17) Knapp, E. W.; Fischer, S. F.; Parak, F. *J. Phys. Chem.* **1982**, *86*, 5042−5047.
(18) Doster, W.; Cusack, S.; Petry, W. *Nature* **1989**, *337*, 754−756.

the conformational substates, and its conformation undergoes almost harmonic motions within the basin of the potential surface. Above the transition temperature, anharmonic motions are observed, owing to the onset of jumping among different substates, which endows a diffusive character to the conformational dynamics. The transition is strongly suppressed in dry proteins,[4] and hence solvent molecules are implicated in the activation of the diffusive anharmonic motions. Such diffusive anharmonic motions were shown to be crucial to the function of a protein ribonuclease A.[16] Collective motions are often inferred to be important for protein function,[19] and a small number of anharmonic collective motions are considered to dominate the total fluctuations.[20] In addition, large-amplitude collective motions characterized by a time scale of $> \sim 0.5$ ps are found to be significantly affected by solvent.[21−23] To find functionally relevant motions and to gain insight into the protein energy landscape, it is useful to determine collective motions from molecular simulation results by principal component analysis (PCA).[20]

Herein, we will show that the protein boson peak originates from a hydration-related multiple minima energy landscape, which is also believed to be the origin of the glasslike transition in proteins.[18] Gaining a detailed understanding of the protein energy landscape is essential not only for determining the origins of the boson peak and glasslike transition but also for elucidating the physicochemical mechanisms involved in protein function. The multiple minima nature of the protein energy landscape is caused not only by the inherent nature of protein itself but also by rearrangement of the atom packing topology between the protein and water molecules, accompanied by large-amplitude collective motions of the protein.[24,25] Solvent molecules are known to affect protein dynamics mainly by two mechanisms. The first is the enhanced anharmonicity, typically emergence of hydration-related multiple minima as mentioned above. This aspect of protein dynamics can be captured well theoretically by the Jumping Among Minima (JAM) model.[23] The second mechanism is the viscosity effect, for example, manifested by damping of vibrational motions.

To study the origin of the protein boson peak, we perform molecular simulations using the atomistic force-field model (AMBER parm99).[26] Inelastic neutron scattering spectra, that is, the incoherent dynamic structure factors, are calculated from the results of simulations. Thus, the relation between atomic fluctuations and neutron scattering spectra is examined. Five types of simulation, normal-mode analysis (NMA), Langevin mode analysis (LMA), molecular dynamics in vacuum (MDV), molecular dynamics simulation with the generalized Born model[27] (MDGB), and molecular dynamics in water (MDW) are applied to hen egg-white lysozyme (PDB code: 4lzt). A boson peak has been observed in neutron scattering experiments of this protein.[3,8] In NMA, the conformational energy surface of the protein is assumed to be a multidimensional parabola. This is an idealized case where neither anharmonicity nor solvent effects are considered. In LMA, viscosity is introduced to NMA, and thus protein motions are expressed as a linear combination of independent Langevin oscillators on the harmonic energy surface.[21−23] In contrast to the above two models, molecular dynamics simulations (MDV, MDGB, and MDW) deal with not only vibrational motion but also anharmonic motion of the protein.[23] In MDGB, solvent is treated as a dielectric continuum instead of explicit water molecules. In our study, MDW gives the most realistic results, including both anharmonicity and solvent effects. In this article, we discuss the relation between the protein energy landscape and the origin of protein boson peak by comparing the results of these simulations.

Methods

Simulation Procedure. In MDV, MDGB, and MDW, the calculation procedure is as follows. After a 150 ps equilibration period, 1 ns MDV, MDGB, and MDW were carried out at 300 K. The 1 ns trajectory was divided into five 200 ps trajectories. From the five structures obtained for every 200 ps simulation over the 1 ns, MDV, MDGB, and MDW were performed at 100 K. Increasing the temperature from 100 K, we performed subsequent simulations at 150, 200, and 250 K using the structure obtained at the end of the previous temperature simulation. Each simulation below 250 K consisted of a 100 ps equilibration period and a 200 ps production period. Physical quantities at each temperature in this paper were calculated as the average of the results from five trajectories.

Hen egg-white lysozyme comprises 1960 atoms in our simulations. In MDW, 8 chloride ions and 7303 water molecules are included in the simulated system, and the AMBER parm99 potential energy function[26] and TIP3P water model[28] are employed. No potential energy cutoff is used in NMA, MDV, and MDGB. In MDW, a periodic boundary condition with a box size of $59.9 \times 67.5 \times 73.7$ Å^3 is imposed, and the particle-mesh Ewald method is used (the Lennard-Jones interactions and the real space Ewald sum are smoothly switched to zero at 10 Å). In MDW, the relative dielectric constant is 1.0. In MDV and NMA, a relative dielectric constant proportional to the distance between atoms is used. The system is weakly coupled to a heat bath by Berendsen's method[29] with a relaxation time of 0.2 ps in order to maintain constant temperature in MDV, MDGB, and MDW. In MDW, Berendsen's method is also used to keep the pressure constant at 1 bar with a relaxation time of 0.2 ps. MDV, MDGB, and MDW are performed with an integration time step of 0.5 fs. In this paper, molecular dynamics simulation and energy minimization for NMA are performed by using the molecular simulation programs AMBER 7[30] and PRESTO,[31] respectively.

Inelastic Neutron Scattering Spectra. Neutron scattering experiments essentially measure the total dynamic structure factor, $S(\boldsymbol{Q},\omega)$, in which $\boldsymbol{Q}$ and ω correspond to the momentum and energy transfers between incident neutron and sample, respectively. Because the incoherent scattering length of hydrogen is 1 order of magnitude larger than the coherent scattering length of all the other atoms in the protein, we assume in this study that their coherent contribution is negligible, that is, $S(\boldsymbol{Q},\omega) \approx S_{\mathrm{inc}}(\boldsymbol{Q},\omega)$. We calculate the incoherent dynamic structure factor, $S_{\mathrm{inc}}(\boldsymbol{Q},\omega)$, as the Fourier transform of a time correlation

(19) Berendsen, H. J. C.; Hayward, S. *Curr. Opin. Struct. Biol.* **2000**, *10*, 165−169.
(20) Kitao, A.; Go, N. *Curr. Opin. Struct. Biol.* **1999**, *9*, 164−169.
(21) Kitao, A.; Hirata, F.; Go, N. *Chem. Phys.* **1991**, *158*, 447−472.
(22) Hayward, S.; Kitao, A.; Hirata, F.; Go, N. *J. Mol. Biol.* **1993**, *234*, 1207−1217.
(23) Kitao, A.; Hayward, S.; Go, N. *Proteins* **1998**, *33*, 496−517.
(24) Kitao, A.; Hirata, F.; Go, N. *J. Phys. Chem.* **1993**, *97*, 10223−10230.
(25) Kitao, A.; Hirata, F.; Go, N. *J. Phys. Chem.* **1993**, *97*, 10231−10235.
(26) Wang, J.; Cieplak, P.; Kollman, P. A. *J. Comput. Chem.* **2000**, *21*, 1049−1074.
(27) Tsui, V.; Case, D. A. *Biopolymers* **2001**, *56*, 275−291.
(28) Jorgensen, W. L.; Chandrasekhar, J.; Madura, J. D. *J. Chem. Phys.* **1983**, *79*, 926−935.
(29) Berendsen, H. J. C.; Postma, J. P. M.; van Gunsteren, W. F.; DiNola, A.; Haak, J. R. *J. Chem. Phys.* **1984**, *81*, 3684−3690.
(30) Case, D. A.; Pearlman, D. A.; Caldwell, T. E.; Cheatham, T. E., III; Wang, J.; Ross, W. S.; Simmerling, T. A.; Darden, T. A.; Merz, K. M.; Stanton, R. V.; Cheng, A. L.; Vincent, J. J.; Crowley, M.; Tsui, V.; Gohlke, H.; Radmer, R. J.; Duan, Y.; Pitera, J.; Massova, I.; Seibel, G. L.; Singh, U. C.; Weiner, P. K.; Kollman, P. A. *AMBER7*; University of California: San Francisco, 2002.
(31) Morikami, K.; Nakai, T.; Kidera, A.; Saito, M.; Nakamura, H. *Comput. Chem.* **1992**, *16*, 243−248.

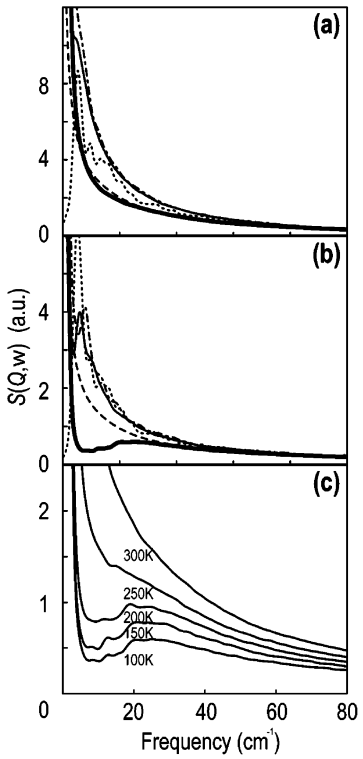

Figure 1. (a and b) Dynamic structure factors, $S(Q,\omega)$, as a function of frequency, ω ($0 < \omega < 80$ cm^{-1}), at $Q = 2.0$ Å^{-1}, calculated using the results of molecular simulations at (a) 300 and (b) 100 K. The results of NMA (· · ·), LMA (- - -), MDV (—), MDGB (- · - · -), and MDW (thick line) are shown. In LMA, we use a friction coefficient of 20 cm^{-1} for all modes. This value is estimated based on calculated values from the literature.[21−23] (c) Temperature dependence of dynamic structure factors, $S(Q,\omega)$, as a function of frequency, ω ($0 < \omega < 80$ cm^{-1}), at $Q = 2.0$ Å^{-1}, calculated using the results of MDW over the temperature range of 100−300 K.

function, that is, the intermediate scattering function, $I_{inc}(\boldsymbol{Q},t)$:

$$S_{inc}(\boldsymbol{Q},\omega) = \frac{1}{2\pi}\int_{-\infty}^{+\infty} dt \exp(-i\omega t) I_{inc}(\boldsymbol{Q},t) \quad (1)$$

$$I_{inc}(\boldsymbol{Q},t) = \sum_j b_{inc,j}^2 \langle \exp(-i\boldsymbol{Q}\cdot\boldsymbol{r}_j(0)) \exp(i\boldsymbol{Q}\cdot\boldsymbol{r}_j(t)) \rangle \quad (2)$$

Here, $b_{inc,j}$ and $\boldsymbol{r}_j$ are the incoherent atomic scattering length and position of atom j, respectively. The functions $I_{inc}(Q,t)$ and $S_{inc}(Q,\omega)$ reported in this paper are the respective averages of $I_{inc}(\boldsymbol{Q},t)$ and $S_{inc}(\boldsymbol{Q},\omega)$ on the sphere $|\boldsymbol{Q}| = Q$. The intermediate scattering functions are calculated from a 200 ps MD trajectory or are analytically calculated in NMA and LMA. In the case of MD, the incoherent dynamic structure factors shown in this paper are averaged over five different trajectories. The function $S_{inc}(Q,\omega)$ is rescaled by the factor $\exp(\hbar\omega/2kT)$ to satisfy the detailed balance condition. Such quasi-classical approximation has been often used in neutron scattering experiments for almost-classical materials.[32] It should be noted that the energy level of kT at 100 K corresponds to a frequency of ~70 cm^{-1}. Therefore, quantum effects are not dominant in the frequency range of the boson peak (~30 cm^{-1}) or lower. To simulate actual experimental resolutions, the inelastic neutron scattering spectra are broadened by convoluting a Gaussian resolution function (width = 1 cm^{-1}).

Results and Discussions

For the simulation results, we first note that the broad peak around 20 cm^{-1} is observed only in the solvated protein at low temperatures below 200 K. At 300 K (Figure 1a), the overall shapes of the incoherent dynamic structure factors, $S(Q,\omega)$, agree with one another at frequencies higher than 70 cm^{-1} but differ at lower frequencies. These results indicate that anharmonicity and solvent effects on protein dynamics can be detected at frequencies lower than ~70 cm^{-1}. This frequency range corresponds to a time scale of >~0.5 ps for the large-amplitude collective motions, which are significantly affected by solvent.[21−23] At this temperature, only the LMA result is in good agreement with that of MDW at frequencies higher than 8 cm^{-1}. Thus, the harmonic model with viscosity can reproduce $S(Q,\omega)$ over a wide frequency range higher than 8 cm^{-1}. The differences in the frequency range lower than 8 cm^{-1} is considered to arise from the anharmonicity of protein energy surface. The calculated results at 100 K (Figure 1b) are significantly different from those at 300 K. The so-called boson peak, a broad peak at around 20 cm^{-1}, is only observed in the MDW result. However, peaks are observed at around 5 cm^{-1} in both NMA and MDV, corresponding to the lowest frequency normal mode. In this respect, MDV behaves very similarly to NMA at 100 K. The shapes of $S(Q,\omega)$ calculated by MDGB are essentially the same as those by MDV at both 300 and 100 K. Thus, the GB model does not take account of either the viscosity effect or the multiple energy minima effect caused by solvent. The effect of viscosity can be observed in the LMA results. In Figure 1b, we see that, when viscosity is introduced, the peak at around 5 cm^{-1} in NMA disappears and instead a single peak is observed at 0 cm^{-1}. Even when examining a range of friction coefficients in LMA, no peak is observed at a finite low frequency. Therefore, the protein boson peak at around 20 cm^{-1} cannot be explained by the effect of viscosity alone. Figure 1c shows the temperature dependence of the incoherent dynamic structure factors calculated using the results of MDW over the temperature range of 100−300 K. This figure reproduces the temperature dependence of $S(Q,\omega)$ observed in inelastic neutron scattering experiments of proteins quite well.[3,4,6]

The behavior of water confined by biological macromolecules at cryogenic temperatures has been reported to differ from that of bulk water.[33] In neutron scattering experiments of solvated proteins at cryogenic temperatures, the system has been shown to be in a metastable state after flash-cooling to 77 K. Water near the proteins in the flash-cooled systems does not crystallize, as the dynamics of the protein and water are thought to be strongly coupled. The temperature control in the present calculations was designed to simulate flash-cooling. To confirm that the water in MDW was not in a solid state even at cryogenic temperatures, we calculated the average number of water molecules hydrogen bonded with each water molecule. Two water molecules were determined as being hydrogen bonded only if their inter-oxygen distance was less than 3.5 Å and their O−H···O angle was larger than 150°. The average values at 100, 150, 200, and 250 K were 1.74, 1.73, 1.72, and 1.69, respectively, and were not largely different from the value of water at 300 K, which is 1.63. Thus, the water was not crystallized and was, in fact, in a supercooled liquid state even at cryogenic temperatures. The water model employed here was TIP3P.[28] The TIP3P model has been widely used to investigate the dynamical properties of solvated proteins at cryogenic temperatures[34] and to obtain the corresponding neutron scattering

(32) Sears, V. F. *Phys. Rev. A* **1985**, *31*, 2525−2533.

(33) Weik, M. *Eur. Phys. J. E* **2003**, *12*, 153−158.

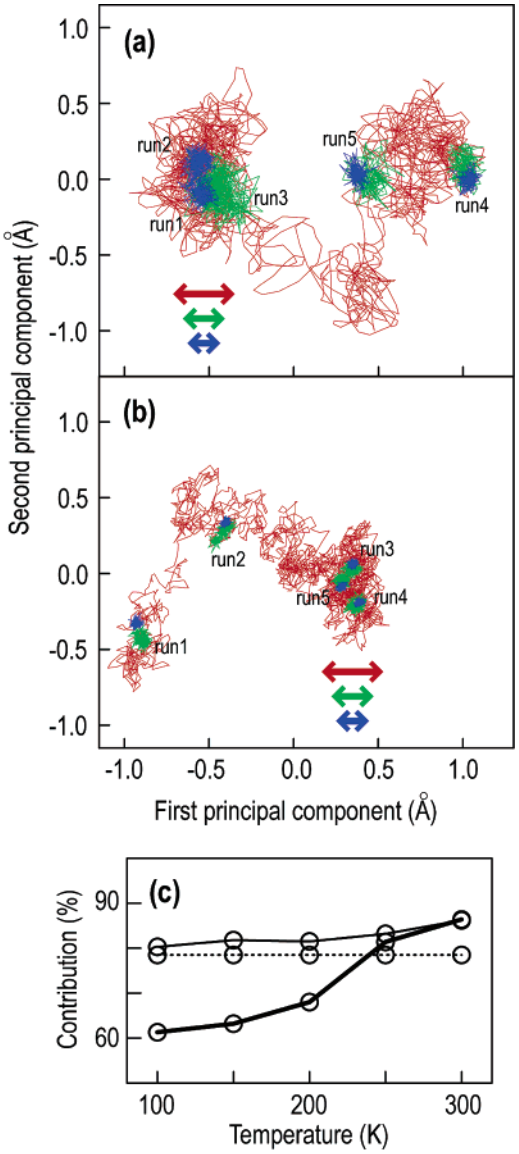

Figure 2. (a) MD trajectories of hen egg-white lysozyme in vacuum projected onto the plane defined by the 1st and 2nd principal components of the 1 ns trajectory at 300 K. (b) Equivalent data in water. The results of simulations at 100 (blue), 200 (green), and 300 K (red) are shown. Five trajectories are plotted in the results of simulations at 100 and 200 K. The projected trajectories are divided by the square root of the total protein mass, and thus have dimensions of angstroms. The magnitudes of the mass-weighted mean-square fluctuations from the lowest frequency mode of NMA at 100 (blue), 200 (green), and 300 K (red) are also indicated by the width of the double-headed arrows. (c) Temperature dependence of the contributions of the first 100 principal components of 200 ps trajectories to the total mass-weighted mean-square fluctuation of the protein. The results of MDV (—) and MDW (thick line) are shown. The contribution of the lowest 100 frequency modes of NMA (· · ·) to the mean-square fluctuation is independent of temperature.

data.[10,35,36] To confirm that our findings do not depend on the water model, we also carried out MDW using the TIP4P[28] model, in which water has been shown to crystallize at low temperatures.[37] The simulated $S(Q,\omega)$ for this model was in good agreement with the results for TIP3P shown in this paper (data not shown).

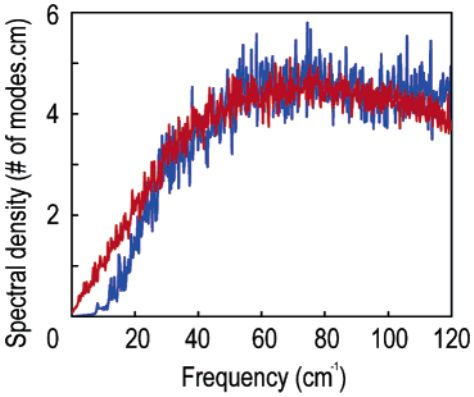

Figure 3. Spectral density from MDW at 300 K (*red line*) and at 100 K (*blue line*) in the frequency range $0 < \omega < 120$ cm^{-1}.

To analyze the protein energy surface over the important subspace spanned by dominant collective coordinates, the trajectories in MDV and MDW at 100, 200, and 300 K are projected onto the plane defined by the 1st and 2nd principal components of each 1 ns trajectory at 300 K (Figure 2). The projections of these trajectories onto the 1st and 2nd principal components at 300 K contribute to the total mean-square fluctuation of atoms (MSF) by 39 and 37% in MDV and MDW, respectively. Those at 200 and 100 K contribute to the total MSF by 34 and 38% in MDV, and 41 and 42% in MDW, respectively, which are not largely different from the contributions at 300 K. Similar to the results of BPTI,[22] the present results show that, at 300 K, lysozyme motion in water (MDW) varies in two ways from that in vacuum (MDV); first, the motion appears to be more diffusive in MDW, and second, the size of clusters observed for the trajectories is smaller in MDW. The diffusive nature of the trajectories in MDW was characterized more clearly by overdamping of the autocorrelation function for each principal component (data not shown) as demonstrated previously.[21−23] As seen in Figure 2, at cryogenic temperatures, the protein motion in water is trapped in a smaller-scale cluster than in vacuum. This means that the protein dynamics are confined to fine structures on the energy surface at low temperatures. Such fine structures have been shown to arise from the existence of structured water molecules around the protein molecule.[25] The temperature dependence of the amplitude of MDV fluctuation along the direction of the collective coordinates in each cluster is almost the same as that expected from NMA below the glasslike transition temperature. Similar results were also observed along the other large-amplitude principal components (data not shown). Furthermore, in MDV below 200 K, the contributions of the first 100 principal components to the total mean-square fluctuation are also in good agreement with those of the lowest 100 frequency (5−30 cm^{-1}) modes of NMA. However, those in MDW below 200 K are much smaller. These results indicate strong suppression of the collective motions in protein in MDW at cryogenic temperatures, while the temperature dependence of the protein fluctuation in MDV can be regarded as harmonic in this low-temperature range.

To summarize, the protein boson peak is observed only in MDW, which indicates that a feature of the dynamics existing in MDW but not in NMA, LMA, MDV, nor MDGB is responsible for the peak. As mentioned earlier, large-amplitude

(34) Vitkup, D.; Ringe, D.; Petsko, G. A.; Karplus, M. *Nat. Struct. Biol.* **2000**, *7*, 34−38.
(35) Loncharich, R. J.; Brooks, B. R. *J. Mol. Biol.* **1990**, *215*, 439−455.
(36) Hayward, J. A.; Smith, J. C. *Biophys. J.* **2002**, *82*, 1216−1225.
(37) Matsumoto, M.; Saito, S.; Ohmine, I. *Nature* **2002**, *416*, 409−413.

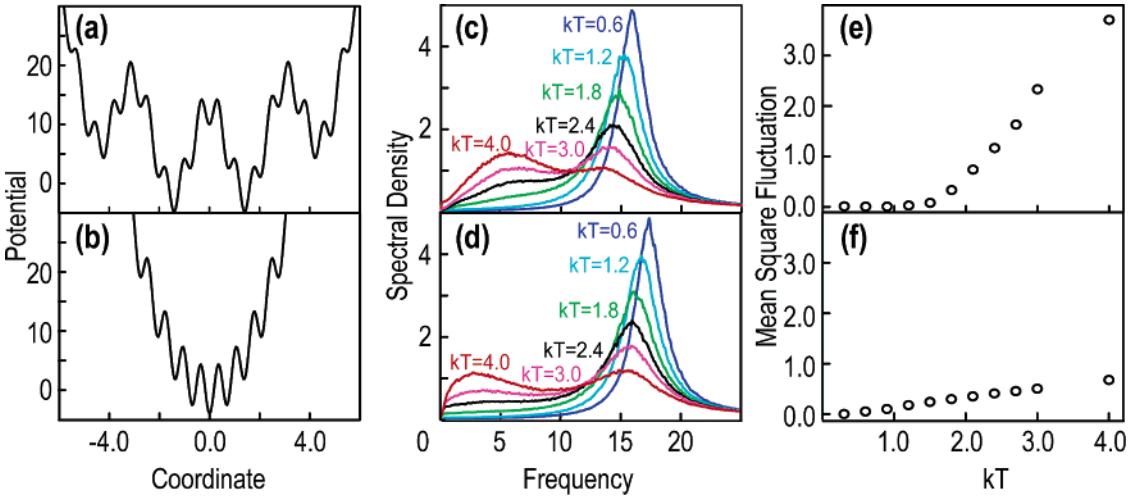

Figure 4. Model one-dimensional (a) multiply hierarchical and (b) singly hierarchical energy surfaces, and results of Brownian dynamics simulation using these surfaces. Power spectral densities for (a) and (b) are shown in (c) and (d), respectively. Temperature dependences of mean-square fluctuations for (a) and (b) are shown in (e) and (f), respectively.

collective motions cause structural changes in the hydrated hydrogen bond network, producing fine local minima on the energy surface. Energy barriers between such minima are relatively low, and at room temperature, jumping among them can occur easily. Such diffusive motions are reflected at the outskirts (5−30 cm^{-1}) of the central quasi-elastic peak. As the temperature is decreased below ∼200 K, the collective motions become trapped in these fine minima, causing the diffusive motions to be replaced by vibrational motions, as reflected in the decrease of density of $S(Q,\omega)$ at the outskirts of the peak. This phenomenon can be confirmed by spectral density calculated as the Fourier transform of the velocity autocorrelation functions at 300 and 100 K (Figure 3). Here, we can clearly see that motions in the frequency range below ∼30 cm^{-1} decrease significantly upon cooling to 100 K. Thus, the diffusive motions at room temperature are produced by motions in this frequency range, which are replaced by vibrational motions at significantly higher frequencies than 100 cm^{-1}. When the ω-dependence of $S(Q,\omega)$ is calculated from the obtained spectral density using a one-phonon approximation, the boson peak shown in Figure 1c at 100 K is precisely reproduced. This quantitatively confirms the predicted mechanism behind the boson peak. Lubchenko and Wolynes explained the origin of the boson peak by using a quantum model, the so-called two-level system.[38] Our view is similar to theirs in the sense that the existence of different energy levels is the origin of the boson peak, although this paper uses a classical treatment as opposed to the quantum treatment of Lubchenko and Wolynes.

Finally, we discuss the number and nature of degrees of freedom involved in the above transition from diffusive motion at room temperature to vibrational motion at cryogenic temperatures. In our previous study,[23] the collective motions in the solute protein are classified into three types. In Type 1, motions on a multiply hierarchical energy surface account for ∼0.5% of the total degrees of freedom. In Type 2, motions on a singly hierarchical energy surface account for ∼4.5% of the total degrees of freedom. In Type 3, harmonic motions account for the remaining 95%. The energy surfaces of Types 1 and 2 are illustrated in Figure 4a and b. Types 1 and 2 collective motions should be involved in the transition and, therefore, responsible for the boson peak. The shift in spectral density from lower to higher frequencies is illustrated in Figure 4c,d. Frequencies below ∼30 cm^{-1} correspond to a time scale of >∼1 ps. Types 1 and 2 collective motions occur in this time scale at room temperature. Although collective motions on a multiply hierarchical energy surface account for less than 0.5% of the total degrees of freedom, they dominate the total fluctuations, contributing by more than 80%. JAM motions along these degrees of freedom are responsible for the glasslike transition. This situation is illustrated in Figure 4e. Since the existence of fine structures on the energy surface is common in glassy materials, we consider that our explanation should apply not only to proteins but also to other materials.

Acknowledgment. This work was supported by a Grant-in-Aid for Young Scientists (B) to Y.J., and Grants-in-Aid for Scientific Research on Priority Areas (C) "Genome Information Science" to A.K., and "Water and Biomolecules" to A.K. and Y.J. from the Ministry of Education, Culture, Sports, Science and Technology of Japan.

JA0425886

(38) Lubchenko, V.; Wolynes, P. G. *Proc. Natl. Acad. Sci. U.S.A.* **2003**, *100*, 1515−1518.